Weckmann, U., Ritter, O., Chen, X., Tietze, K., de Wit, M. (2012): Magnetotelluric image linked to surface geology across the Cape Fold Belt, South Africa. - *Terra Nova*, *24*, 3, pp. 207—212.

DOI: http://doi.org/10.1111/j.1365-3121.2011.01054.x

Journal Name	Manuscript No.	B	Dispatch: 26.12.11	Journal: TER	CE: Bharani
TER	10544		Author Received:	No. of pages: 6	PE: Revathi

doi: 10.1111/j.1365-3121.2011.01054.x

Magnetotelluric image linked to surface geology across the Cape Fold Belt, South Africa

Ute Weckmann,[1] Oliver Ritter,[1] Xiaoming Chen,[1] Kristina Tietze[1] and Maarten de Wit[2]

[1]*Helmholtz Centre Potsdam, German Research Centre for Geosciences GFZ, Telegrafenberg, 14473 Potsdam, Germany;* [2]*Geosciences and AEON – Africa Earth Observatory Network, Nelson Mandela Metropolitan University, Port Elizabeth, South Africa*

ABSTRACT

The subsurface structure of the Cape Fold Belt (CFB) that traverses southern Africa remains largely unknown because it lacks deep-penetrating, high-resolution geophysics. This hampers studies from local-scale exploration for important resources such as water, to continental-scale modelling, such as Gondwana reconstructions. Our Magnetotelluric (MT) soundings across the CFB provide a high-resolution crustal-scale electrical conductivity image. Inversion models of these data correlate well with surface geology, and resolve deep resistive roots of the CFB's regional Palaeozoic quartzite ridges (Swartberg and Outeniqua Mountains) and thin tectonic wedges of Proterozoic rocks of higher resistivity (Kango and Kaaimans Inliers), separated by 2–3 km of Cretaceous sediments in asymmetric intermontaine basins. One of these basins, the Oudtshoorn Basin, is flanked by a listric normal fault rooted in an upper crustal detachment zone, and is underlain by a massive conductivity anomaly that is likely to be a major saline water reservoir.

Terra Nova, 00, 1–6, 2011

Introduction

The Cape Fold Belt (CFB) is a major Phanerozoic African structure that has been studied for more than a century to test Gondwana reconstructions (Reeves and de Wit, 2000; Milani and de Wit, 2008; de Wit *et al.*, 2008). Despite these geological studies, the structure and evolution of the CFB remains controversial (e.g. Shone *et al.*, 1990; Newton *et al.*, 2006; Paton, 2006; Tankard *et al.*, 2009; Booth, 2011). Recent regional refraction- and tele-seismic experiments reveal only general crustal thickness variations, but poorly define internal structures beneath the CFB (Paton, 2006; Stankiewicz *et al.*, 2008; Parsiegla *et al.*, 2009). This hampers further understanding of the structure and evolution of the CFB and tests for more robust links to other Gondwana continents (Milani and de Wit, 2008).

Herein, we report on a magnetotelluric (MT) experiment carried out in November 2005 across the CFB that, for the first time, robustly links surface geological structures down to depths of ca. 10–15 km. The location of the MT profile allows the construction of an upper crustal conductivity section across the CFB from its northern tectonic front to its southernmost coastal ranges.

Correspondence: Ute Weckmann, Helmholtz Centre Potsdam, German Research Centre for Geosciences GFZ, Telegrafenberg, 14473 Potsdam, Germany. Tel.: +49 (0)3312882824; fax: +49 (0)3312881266; e-mail: ute.weckmann@gfz-potsdam.de

Geology and tectonic setting

The CFB formed in response to subduction-related compression during Paleozoic–Mesozoic convergence along the southwestern margin of Gondwana resulted in a coupled CFB-Karoo Foreland Basin (Hälbich, 1983; Milani and de Wit, 2008; Tankard *et al.*, 2009; Lindeque *et al.*, 2011). The main deformation took place at ca. 250 Ma. This tectonism affected Proterozoic metasediments and an unconformably overlying Palaeozoic cover (Fig. 1). Crystalline Proterozoic basement is not exposed anywhere in the CFB. In the study area, the Proterozoic metasediments are exposed in tectonic windows known as the Kango and Kaaimans Inliers that range in age between ca. 520 and 1050 Ma (Barnett *et al.*, 1997). Lower Cambrian granite intrudes the Kaaimans Group (Fig. 1). Unconformably overlying these rocks and making up the highest mountain ranges of the CFB are predominantly thick dense quartzite units of the lower Paleozoic Cape Supergroup (Table Mountain and Witteberg Groups). These prominent ranges, which outcrop for hundreds of kilometres along the strike of the CFB, are separated by softer Silurian–Devonian shales (Bokkeveld Group) exposed mostly in the adjacent valleys. Permo-Carboniferous tillites (Dwyka Group) and finer siliciclastic rocks of the Permo-Triassic Karoo Supergroup make up the uppermost sequences, but these are preserved predominantly only in the Karoo foreland basin (Johnson *et al.*, 1997; Fildani *et al.*, 2009).

Our MT-line across the CFB runs close to an amphibian seismic refraction profile (Stankiewicz *et al.*, 2008; Parsiegla *et al.*, 2009) that reveals a steep decrease in crustal thickness from ca. 42 km below the tectonic front of the CFB (at the Swartberg Mountains) to ca. 30 km below the coastal ranges. A high-velocity mid-lower crust probably comprises Mesoproterozoic crystalline basement (Stankiewicz *et al.*, 2008). The Swartberg and the Outeniqua Mountains display slow p-wave velocities down to about 2 km depth, similar to the Kango and Kaaimans metasediments within the uppermost 1 km of the crust.

Cretaceous basins, located alongstrike of the CFB at the east coast, are known to project westward into the intermontaine basins of the CFB (Dingle *et al.*, 1983; Brown *et al.*, 1995; Paton, 2006). The correlations reveal that the normal south-dipping listric fault systems separate the onshore Cretaceous basins from the Proterozoic inliers with displacements of 2–6 km (e.g. the Worcester and Kango Faults). Paton (2006)

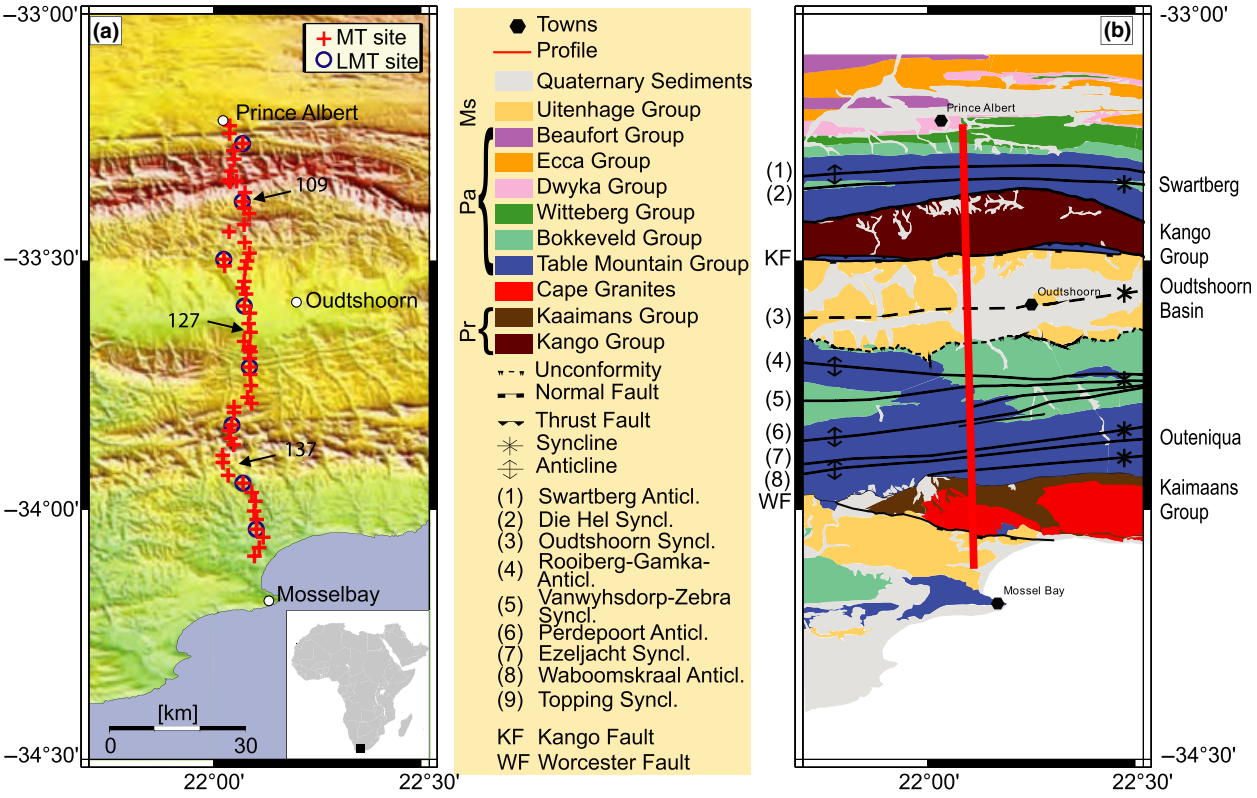

Fig. 1 (a) Location map of the MT sites along the transect through the CFB. Red crosses indicate broadband MT sites; blue circles indicate combined broadband and long period MT sites. (b) Geological map of the study area (1:250 000 geological map 3322, Oudtshoorn. Geoscience Council, Pretoria, RSA). The profile (red line) crosses the Oudtshoorn Basin and the Kango and the Kaaimans inliers, as well as the Swartberg and the Outeniqua Mountains. Pr: Proterozoic, Pa: Palaeozoic, Ms: Mesozoic.

speculated that these faults are linked at mid-crustal depths to a mega-extensional detachment fault underlying the entire CFB and increasing in depth from ~10 km beneath the CFB tectonic front to about 30 km near the coast (i.e. close to Moho depths). Paton further speculated that above these Cretaceous normal faults systems exploited earlier Paleozoic thrusts systems and that the CFB changed from being a 'thick-skinned' belt beneath the coastal ranges to a 'thin-skinned' belt closer to its tectonic front. Farther north, the thrusts apparently extend into the adjacent Karoo Basin (Paton, 2006) where shallow (2–3 km depth) décollements have been mapped using a seismic reflection profile across the Karoo Basin (Lindeque *et al.*, 2011). Other authors have suggested instead that the junction between the CFB and the Karoo Basin is a steeply dipping crustal transform fault that effectively decoupled these two tectonic domains (Johnston, 2000; Tankard *et al.*, 2009). Tankard *et al.* (2009) further suggest that intermontaine listric Kango and Worchester Faults are part of transpressional flower structures, including the Kango and the Kaaimans inliers and their bounding mountain ranges. Such a model requires a depth extent of ~8 km for the inliers, and 6–11 km for the Outeniqua and Swartberg Mountains respectively (Tankard *et al.*, 2009). These widely different models serve as examples to emphasize the lack of consensus about even the simplest geometry of the upper crustal structures that underlie the CFB, and therefore its tectonic evolution. We use our MT data to test some of these controversies.

Magnetotelluric data and inversion results

Magnetotelluric data were recorded at 52 stations spaced at 2 km intervals along a 100-km long section across the CFB (Fig. 1). Such spacing facilitates high-resolution MT modelling compared with the typical ~10 km spacing for regional surveys (e.g. Jones *et al.*, 2009), which is a proxy for spatial resolution.

Electric and magnetic field variations (1 kHz–1 mHz) were measured using S.P.A.M. MkIII and CASTLE instruments, Metronix induction coils and Ag/AgCl and processed according to Ritter *et al.* (1998) and Weckmann *et al.* (2005). Figure 2 shows examples of data together with model responses for three sites, 137, 127 and 109 (c.f. Fig. 1 for locations).

MT data inversion results yield several prominent conductive and resistive features (Fig. 3 – (c1–c5) and (r1–r4) respectively). Resistor r1 is located beneath the Swartberg Mountains and extends to a depth of ~10 km, enclosing a thin shallow conductive feature (c5). Flanking the Swartberg Mountains to the south, we observe a shallow, south-dipping wedge (r2) with resistivities of 5000 Ωm and a thickness of ~2 km.

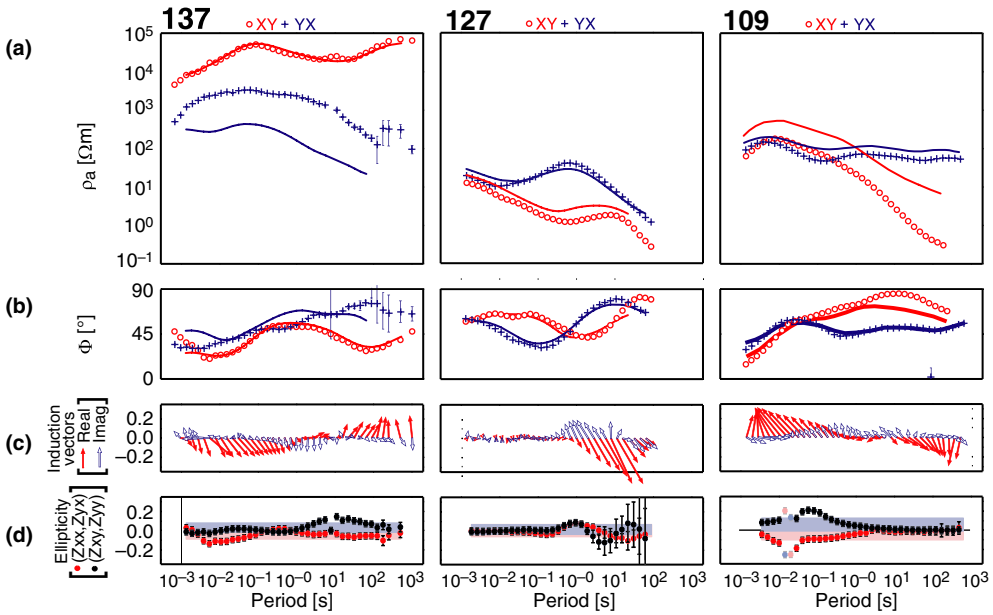

Fig. 2 MT data (markers) and model response (solid lines) of three MT sites along the profile. The upper two panels show the apparent resistivities and phases of both off-diagonal components. The apparent resistivities are generally higher where a station is located in the mountain ranges (e.g. sites 137 and 109) and lower if a site is located in one of the valleys (e.g. site 127). Apparent resistivities exhibit the influence of *static shift* caused by charge accumulations at boundaries of shallow heterogeneities. Phases and the shape of the apparent curves conform well with the 2D model. At some stations in the area of the Oudtshoorn Basin, we observe phases leaving the first quadrant at low frequencies (<0.01 Hz). This is probably caused by electrical anisotropy (Weckmann *et al.*, 2003). We therefore exclude such data (xy-component <0.02 Hz at five central sites) from 2D inversion. The third panel displays the real and imaginary part of the vertical magnetic transfer function as induction vectors (Wiese convention, Wiese, 1962). Real induction vectors predominantly point in north or south directions, indicating E-W striking conductivity structures, consistent with the general structural trends in the CFB. The bottom panel shows ellipticities obtained from the decomposition method after Becken and Burkhardt (2004). Vanishing ellipticities are in agreement with regional 2D conditions, whereas larger ellipticities indicate 3D effects. Shaded areas indicate confidence limits. This analysis provides independent estimates of the geo-electric strike direction derived from the MT impedance tensor data. After rotating the MT data by −90°, the xy-component represents the TE mode (electric field parallel to the geo-electric strike direction) and the yx-component of the TM mode (electric field perpendicular to the geo-electric strike direction).

A third resistive structure (r3) extends to ~4 km depth beneath the Outeniqua Mountains.

The most prominent feature in the model section is the high-conductivity body c1 centred beneath the Oudtshoorn Basin, with resistivity values of less than 1 Ωm. The well-resolved top of c1 (Fig. 3) lies between 3 km and 4 km below surface and can be traced along a horizontal distance of ~40 km. The conductor requires a minimum thickness of 4–5 km to fit the data, but the bottoms of conductive structures are poorly resolved with MT. Laterally, c1 clearly reaches far beyond the surface expression of the Oudtshoorn Basin, deepening slightly beneath the Kango inlier to the north. It also extends towards the south beneath the surface outcrops of open-folded Bokkeveld shales, where it appears to terminate along a sub-vertical surface that apparently reaches close to Earth's surface along an inferred steep fault.

Several isolated shallow conductive features (c3, c4) are located in the upper 2 km of the crust. These may represent conductive layers in the Cretaceous sediments of the Oudtshoorn Basin. Farther south, a conductive feature (c2, ~10 Ωm) located beneath the resistive roots of the Outeniqua Mountains at ~10 km depth appears to connect to shallower levels at profile kilometre 35.

Discussion

Visual comparison between the surface geology and the resistivity image reveals some striking coincidence between lateral variations in electrical conductivity and abrupt changes in the geology (e.g. black arrows in Fig. 4). The Swartberg Mountains, for example, appear in the resistivity section as a sub-vertical resistive zone extending to a depth of 10 km with a shallower wedge of high conductivities (c5 in Fig. 3) that at surface has been mapped as a syncline of Bokkefeld shales.

At surface, the geology of this range comprises almost entirely a sub-vertical to steeply overturned section of Table Mountain Group (TMG) quartzites, with a small centrally embedded, shallow-plunging synform (with a vertical axial plane) of Bokkeveld shales. The Kango inlier appears as a resistive wedge that continues southward to ~5 km depth beneath the poorly consolidated terrestrial sediments (conglomerates, sandstones and shales) of the Oudtshoorn Basin that has a stratigraphic thickness of 2–3 km (Dingle *et al.*, 1983). The Kango

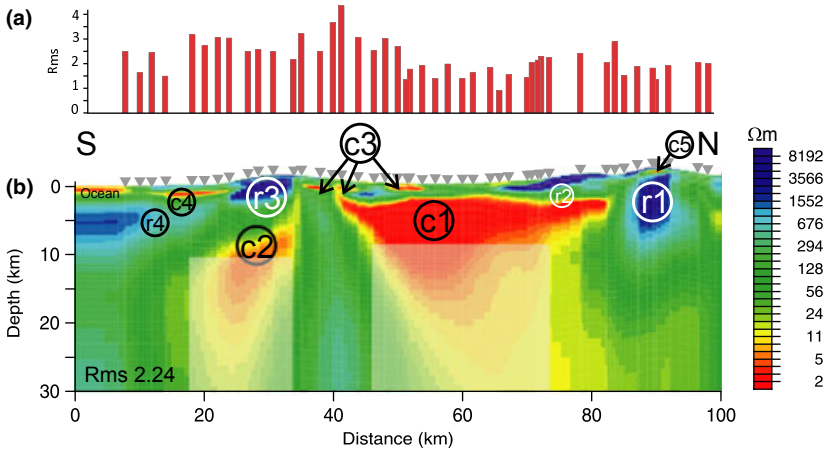

Fig. 3 Data fit at individual sites (a) for 2D inversion model (b) of the 100 km long transect through the CFB on a crustal scale (upper 30 km) obtained by 2D inversion of the TE, TM and the induction vector data using the RLM2DI algorithm (Rodi and Mackie, 2001). Inversion started from a homogenous half-space with a mesh of 235 horizontal and 174 vertical cells. The regularization parameter τ, which controls the trade-off between data misfit and model roughness, was chosen to be 15 after computing a trade-off for different τ values. Error bounds were set to 0.01 for the vertical magnetic transfer function, to 0.6° for the TE and TM phases, to 10% for the TM and 100% for the TE apparent resistivities. The increased error bounds for TE apparent resistivities were necessary to accommodate static shift effects. Zones of high electrical conductivity appear in red, whereas resistive zones are indicated in blue. Several very prominent conductivity anomalies, labelled c1–c5 and r1–r4. The shallow conductive feature c5 provides a relative scale for the excellent resolution quality of the MT data. Resolution tests, using model modifications and comparison of respective data fits were applied to evaluate the significance, extent and resolution of the conductivity features.

rocks and a thin sliver of unconformably overlain TMG quartzites (Fig. 1) are separated from the Oudtshoorn Basin by the Kango Fault. The listric nature of the fault is well displayed in outcrop (Paton, 2006). The conductivity model (Fig. 3) images the Kango fault indirectly as a juxtaposition of these different lithologies, and the fault appears to follow a shallow southward dip (< 20°) that can be traced down to 2–3 km. This does not support the Kango Fault being a high angle fault as part of a transpressional flower structure (Tankard *et al.*, 2009), or penetrating as deep as 10 km (Stankiewicz *et al.*, 2008). The MT data are also not consistent with a depth extent of the Kango inlier to 8 km as proposed by Tankard *et al.* (2009). A shallow Kango fault, as suggested by the resistivity section, is more compatible with thin-skinned tectonics. Although Paton (2006) draws a possible transition to predominantly thin-skinned tectonics to the north of the Swartberg region, the Kango Fault clearly dips less steeply than previously assumed. Thus, a possible detachment zone may be located much farther south at a shallow depth of < 2–3 km, and the Kango inlier may even be allochthonous.

The Oudtshoorn Basin is imaged with intermediate (~40 Ωm) resistivities to a depth of 2–3 km in its centre. This is in excellent agreement with geological observations (Dingle *et al.*, 1983). Both the Oudtshoorn Basin and the Kango inlier are underlain by a massive zone of high conductivity, with an upper boundary at 3–4 km below surface and from there extending down to at least 7 km depth. To explain the high electrical conductivities, electrically conducting material must be interconnected over large distances. Possible candidates include mineralized phases such as disseminated sulphides or ore deposits. These are common in the Mesoproterozoic crystalline basement Namaqualand (Ryan *et al.*, 1986). However, as the depth to crystalline basement beneath the Oudtshoorn Basin occurs at about 8–10 km (Stankiewicz *et al.*, 2008), it remains unlikely that the anomaly occurs in the basement. Alternatively, a thickness of up to 1 km of Bokkeveld shales and ca. 2 km of Peninsula quartzites can be inferred to exist directly beneath the Oudtshoorn Basin, calculated from the anticline–syncline structures in the adjacent Cape Supergroup rock south and east of the basin. The intermediate resistivities in the section are consistent with those of the Bokkeveld shales at the surface, although these are likely to be thin (< 1 km) or even absent beneath the Outdshoorn Basin (Dingle *et al.*, 1983). The observed high-conductivity anomaly therefore most likely lies within the TMG quartzites, which are known to be fractured and to host major aquifers in the vicinity of Oudtshoorn (Umvoto Africa, 2005). In that case, highly fractured TMG and possibly Kango Group quartzites filled with saline fluids could also explain this large, prominent conductive anomaly. Towards the southern end of this anomaly, we note a sub-vertical conductor reaching close to the surface. Hot springs exist near the village of Warmbad (i.e. warm-bath, Fig. 4). The shallow patch of high conductivity near the surface could be related to fluids originating at a depth of ~1 km, and may be an expression of a fluid pathway along a subvertical fault zone connecting to a larger fluid reservoir at greater depth.

The Outeniqua Mountains appear as a resistive zone reaching a depth of approximately 5 km. This is in general agreement with structural analyses of Hälbich (1983) that predicts a regional synform, but not with a proposed flower structure (Tankard *et al.*, 2009). The resistive feature (r3) correlates spatially with the TMG quartzites within the mapped regional synclinorium (Fig. 1b). Beneath the Outeniqua Mountains, we also observe a deep (> 8 km) zone of high electrical conductivity (c2) bound on the north by a sub-vertical structure that reaches to shallower levels of approximately 5 km depth. To the south, the Kaaimans Group is expressed by intermediate conductivities (~400 Ωm) in the upper 1 km of the crust, underlain by a thin layer of high electrical conductivities. Deeper than 3 km, we observe a more resistive

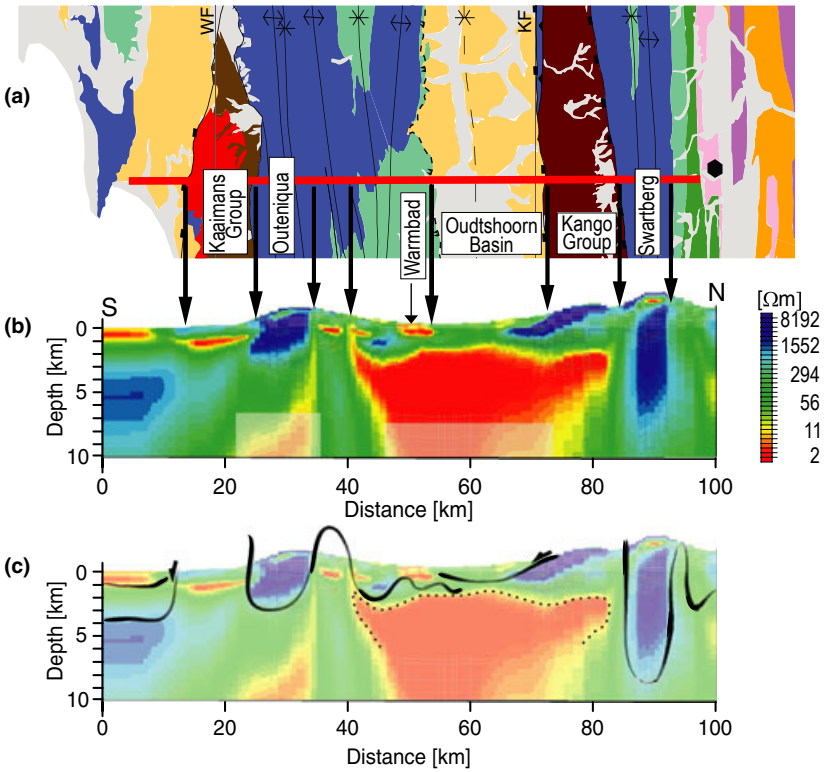

Fig. 4 Comparison of (a) the geological map from Fig. 1b with the (b) upper 10 km of the MT resistivity section. Black arrows indicate surface traces of known faults and/or distinct lithological boundaries that correlate with the location of distinct electrical conductivity changes. (c) Sketch of the interpretation of the conductivity features and location of faults and the potential saline water reservoir (dotted).

structure that seems to continue southwards beneath the Indian Ocean. Compared with the Kango rocks, the Kaaimans inlier appears to be less resistive. This could be related to significant lithological differences between the two inliers. For instance, the Kango inlier includes major carbonate sequences that are not present in the Kaaimans inlier, whereas the latter is intruded by significant volumes of granite that are absent in the Kango. Despite these differences in geologic make up, both inliers are imaged as relatively shallow, wedge-shaped resistive units underlain by more conductive material, and may well be allochtonous, although this would need to be confirmed with data.

Conclusion

An electrical section across the CFB indicates that much of its surface geology can be linked with confidence to subsurface structures of the upper crust using MT techniques. The MT data are able to resolve what are interpreted as regional sub-horizontal décollement structures shaped during compressional and extensional tectonics that have formed this belt over a period of more than 100 Ma. The MT image can distinguish the major Paleozoic rock units of the CFB, and shows that its Proterozoic inliers probably are part of thin tectonic wedges. It also confirms that the CFB's Cretaceous intermontaine basins are bound by regional shallow listric faults that reflect thin-skinned tectonism and are not subvertical transpressional zones. Recognition that most of the important structural discontinuities exposed in the CFB link to shallow dipping décollements, makes them unsuitable for use in Gondwana reconstructions (cf. de Wit *et al.*, 2008). Finally, major high-conductivity anomalies in the upper crust beneath the CFB, in particular, beneath the Oudtshoorn region, may represent large undiscovered saline water reservoirs. If confirmed through drilling, these could serve this water-poor area in future – e.g. as a source for shale gas exploration (de Wit, 2011).

Acknowledgements

Fieldwork in South Africa was funded by the Deutsches GeoForschungsZentrum. The Geophysical Instrument Pool Potsdam provided the MT equipment. This experiment would not have been possible without the dedicated support of Rod Green and Albert Alchin, and financial support in South Africa from the Department of Science and Technology and the National Research Foundation. We thank Wilgewandel resort, and all farmers for permitting access to their properties and our German and South African students and colleagues for their assistance in the field. UW was supported by the Emmy Noether fellowship of the German Science Foundation DFG. Reviews by Mark Muller, Nicole Grobys and an anonymous reviewer are greatly appreciated. This is *Inkaba yeAfrica* contribution number 65, and AEON contribution number 98.

References

Barnett, W., Armstrong, R.A. and de Wit, M.J., 1997. Stratigraphy of the upper Neoproterozoic Kango and lower Paleozoic Table Mountain Group of the Cape Fold Belt revisited. *S. Afr. J. Geol.*, **100**, 237–250.

Becken, M. and Burkhardt, H., 2004. An ellipticity criterion in magnetotelluric tensor analysis. *Geophys. J. Int.*, **159**, 69–82.

Booth, P., 2011. Stratigraphic, structural and tectonic enigmas associated with the Cape Fold Belt: challenges for the future. Inkaba yeAfrica Special volume 2. *S. Afr. J. Geol.*, **???**, ???–???. in press.

Brown, L.F. Jr, Benson, J.M., Brink, G.J., Doherty, S., Jollands, A., Jungslager, E.H.A., Keenan, J.H.G., Muntingh, A. and van Wyk, N.J.S., 1995. Sequence stratigraphy in Offshore South African divergent basins: an atlas on exploration for Cretaceous lowstand traps by Soekor (Pty) Ltd. *AAPG Stud. Geol.*, **41**, 184.

Dingle, R.V., Siesser, W.G. and Newton, A.R., 1983. *Mesozoic and Tertiary Geology of Southern Africa*, A. A. Balkema, Rotterdam, 375.

Fildani, A., Weislogel, A., Drinkwater, N.J., McHargue, T., Tankard, A., Wooden, J., Hodgson, D. and Flint, S., 2009. U-Pb zircon ages from the southwestern Karoo Basin, South Africa – Implications for the Permian-Triassic boundary. *Geology*, **37**, 719–722.

Hälbich, I.W., 1983. A geodynamic model for the Cape Fold Belt. In: *Geodynamics of the Cape Fold Belt* (A.P.G. Söhnge and I.W. Hälbich, eds), pp. 177–184.

Geological Society of South Africa,????????. Special Publication No.12.

Johnson, M.R., Van Vuuren, C.J., Visser, J.N.J., Cole, D.I., de Wickens, H.V., Christie, A.D.M. and Roberts, D.L., 1997. The foreland Karoo Basin, South Africa. In: *Sedimentary Basins of the World*, **Vol. 3** (R.C. Selley, eds). pp. 269–317. African Basins, ?????????.

Johnston, S.T., 2000. The Cape Fold Belt and Syntaxis and the rotated Falkland Islands: dextral transpressional tectonics along the southwest margin of Gondwana. *J. Afr. Earth Sci.*, **31**, 51–63.

Jones, A.G., Evans, R.L. and Eaton, D.W., 2009. Velocity–conductivity relationships for mantle mineral assemblages in Archean cratonic lithosphere based on a review of laboratory data and Hashin–Shtrikman extremal bounds. *lithos*, **109**, 131–143.

Lindeque, A., de Wit, M.J., Ryberg, T., Weber, M. and Chevallier, L., 2011. Deep crustal profile across the southern Karoo Basin and Beattie Magnetic Anomaly, South Africa: an integrated interpretation with tectonic implications. *S. Afr. J. Geol.*, **???**, ????–????. in press

Milani, E.J. and de Wit., M.J., 2008. Correlations between classic Parana and Cape-Karoo basins of South America and southern Africa and their basin infills flanking the Gondwanides: Du Toit revisited. In: *West Gondwana: Pre-Cenozoic Correlations Across the South Atlantic Region*. (R.J. Pankhurst, R.A.J. Trouw, B.B. de Brito Neves and M.J. de Wit, eds), pp. 319–342. Geological Society, London, Special Publications, ????????. 294.

Newton, A.R., Shone, R.W. and Booth, P.W.K., 2006. The Cape Fold Belt. In: *The Geology of South Africa* (M.R. Johnson, C.R. Anhaeusser and R.J. Thomas, eds), pp. 521–530. Geological Society of South Africa/Council for Geoscience, ????????.

Parsiegla, N., Stankiewicz, J., Gohl, K., Ryberg, T. and Uenzelmann-Neben, G., 2009. Southern African continental margin: dynamic processes of a transform margin. *Geochem. Geophy. Geosy.*, **10**, Q03007. doi:10.1029/2008GC002196.

Paton, D.A., 2006. Influence of crustal heterogeneity on normal fault dimensions and evolution: southern South Africa extensional system. *J. Struct. Geol.*, **28**, 868–886.

Reeves, C. and de Wit, M.J., 2000. Making ends meet in Gondwana: retracing the transforms of the Indian Ocean and reconnecting continental shear zones. *Terra Nova*, **12**, 272–280.

Ritter, O., Junge, A. and Dawes, G.J.K., 1998. New equipment and processing for magnetotelluric remote reference observations. *Geophys. J. Int.*, **132**, 535–548.

Rodi, W. and Mackie, R.L., 2001. Nonlinear conjugate gradients algorithm for 2D magnetotelluric inversion. *Geophysics*, **66**, 174–187.

Ryan, P.J., Lawrence, A.L., Lipson, R.D., Moore, J.M., Paterson, A., Stedman, D.P. and Van Zyl, D., 1986. The Aggeneys base metal sulphide deposits, Namaqualand district. In: *Mineral Deposits of Southern Africa*. (C.R. Anhaeusser and S. Maske, eds), 1447–1474. Special Publication of the Geological Society of South Africa, ??????.

Shone, R.W., Nolte, C.C. and Booth, P.W.K., 1990. Pre-Cape rocks of the Gamtoos area – a complex tectono-stratigraphic package preserved as a horst block. *S. Afr. J. Geol.*, **93**, 616–621.

Stankiewicz, J., Parsiegla, N., Ryberg, T., Gohl, K., Weckmann, U., Trumbull, R. and Weber, M., 2008. Crustal Structure of the Southern Margin of the African Plate: results from geophysical experiments. *J. Geophys. Res.*, **113**, ????–????. doi:10.1029/2008JB005612

Tankard, A., Welsink, H., Aukes, P., Newton, R. and Stettler, E., 2009. Tectonic evolution of the Cape and Karoo basins of South Africa. *Mar. Petrol. Geol.*, **26**, 1379–1412.

Umvoto Africa, 2005. Deep artesian groundwater for the oudtshoorn municipal supply. Water Research Commission, WRC Report No. 1254/1/05.

Weckmann, U., Ritter, O. and Haak, V., 2003. A magnetotelluric study of the Damara Belt in Namibia 2 MT phases over 90° reveal the internal structure of the Waterberg Fault/Omaruru Lineament. *Phy. Earth Planet. Inter.*, **138**, 91–112.

Weckmann, U., Magunia, A. and Ritter, O., 2005. Effective noise separation for magnetotelluric single site data processing using a frequency domain selection scheme. *Geophys. J. Int.*, **161**, 635–652.

Wiese, H., 1962. Geomagnetische Tiefentellurik Teil II: Die Streichrichtung der Untergrundstrukturen des elektrischenWiderstandes, erschlossen aus geomagnetischen Variationen. *Geofis. Pura e Appl.*, **52**, 83–103.

de Wit, M.J., 2011. The great shale debate of the Karoo. *S. Afr. J. Sci.*, **107**, (7/8), 1–9.

deWit M.J. and Ransome, I.G.D., (eds) 1992. *Inversion tectonics of the Cape Fold Belt, Karoo and Cretaceous basins of southern Africa.*, A.A. Balkema, Rotterdam, 269.

de Wit, M.J., Stankiewicz, J. and Reeves, C., 2008. Restoring Pan-African-Brasiliano connections: more Gondwana control, less Trans-Atlantic corruption. In: *West Gondwana: Pre-Cenozoic Correlations Across the South Atlantic Region*. (R.J. Pankhurst, R.A.J. Trouw, B.B. de Brito Neves, de. Wit and M. J, eds), 399–412. Geological Society, London, Special Publications,??????. 294,

Received 24 June 2010; revised version accepted 8 December 2011

Author Query Form

Journal: TER

Article: 1054

Dear Author,
During the copy-editing of your paper, the following queries arose. Please respond to these by marking up your proofs with the necessary changes/additions. Please write your answers on the query sheet if there is insufficient space on the page proofs. Please write clearly and follow the conventions shown on the attached corrections sheet. If returning the proof by fax do not write too close to the paper's edge. Please remember that illegible mark-ups may delay publication.

Many thanks for your assistance.

Query reference	Query	Remarks
1	**AUTHOR: Please provide the volume number, page range for reference Booth (2011).**	
2	**AUTHOR: Please provide the city location of publisher for reference Hälbich (1983).**	
3	**AUTHOR: Please provide the city location of publisher for reference Johnson *et al.*** (1997).	
4	**AUTHOR: Please provide the volume number, page range for reference Lindeque *et al.*** (2011).	
5	**AUTHOR: Please provide the city location of publisher for reference Milani and de Wit. (2008).**	
6	**AUTHOR: Please provide the city location of publisher for reference Newton *et al.*** (2006).	
7	**AUTHOR: Please provide the city location of publisher for reference Ryan *et al.*** (1986).	
8	**AUTHOR: Please provide the page range for reference Stankiewicz *et al.*** (2008).	
9	**AUTHOR: de Wit and Ransome (1992) has not been cited in the text. Please indicate where it should be cited; or delete from the Reference List.**	
10	**AUTHOR: Please provide the city location of publisher for reference de Wit *et al.*** (2008).	

USING e-ANNOTATION TOOLS FOR ELECTRONIC PROOF CORRECTION

Required software to e-Annotate PDFs: Adobe Acrobat Professional or Adobe Reader (version 8.0 or above). (Note that this document uses screenshots from Adobe Reader X)
The latest version of Acrobat Reader can be downloaded for free at: http://get.adobe.com/reader/

Once you have Acrobat Reader open on your computer, click on the Comment tab at the right of the toolbar:

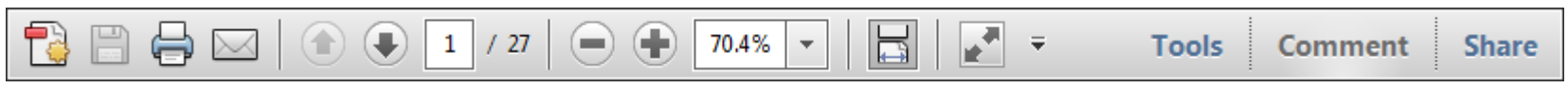

This will open up a panel down the right side of the document. The majority of tools you will use for annotating your proof will be in the Annotations section, pictured opposite. We've picked out some of these tools below:

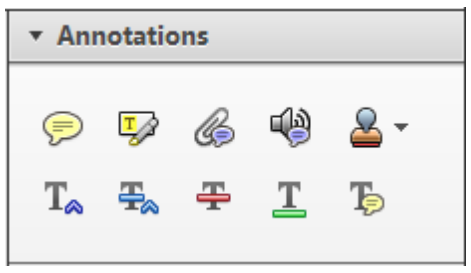

1. Replace (Ins) Tool – for replacing text.

Strikes a line through text and opens up a text box where replacement text can be entered.

How to use it

- Highlight a word or sentence.
- Click on the Replace (Ins) icon in the Annotations section.
- Type the replacement text into the blue box that appears.

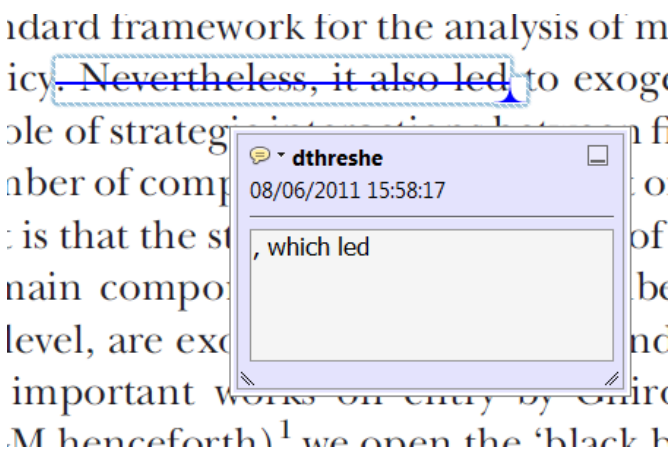

2. Strikethrough (Del) Tool – for deleting text.

Strikes a red line through text that is to be deleted.

How to use it

- Highlight a word or sentence.
- Click on the Strikethrough (Del) icon in the Annotations section.

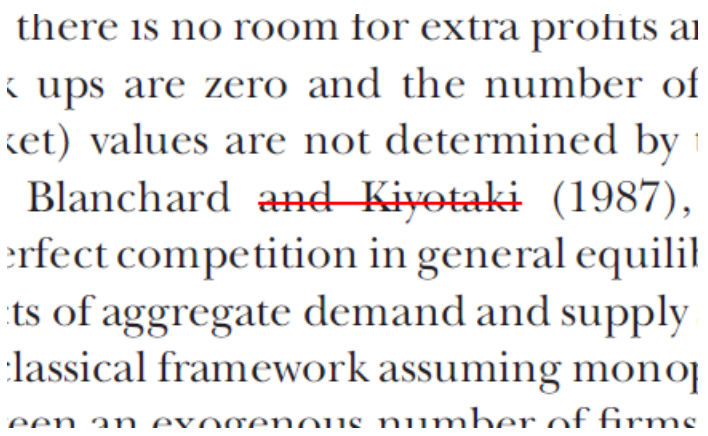

3. Add note to text Tool – for highlighting a section to be changed to bold or italic.

Highlights text in yellow and opens up a text box where comments can be entered.

How to use it

- Highlight the relevant section of text.
- Click on the Add note to text icon in the Annotations section.
- Type instruction on what should be changed regarding the text into the yellow box that appears.

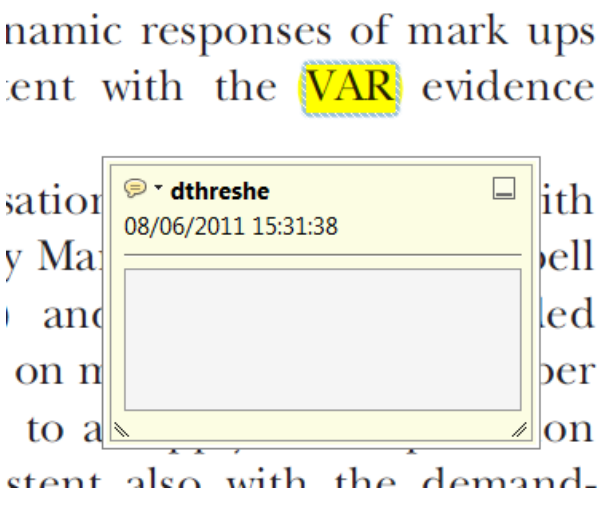

4. Add sticky note Tool – for making notes at specific points in the text.

Marks a point in the proof where a comment needs to be highlighted.

How to use it

- Click on the Add sticky note icon in the Annotations section.
- Click at the point in the proof where the comment should be inserted.
- Type the comment into the yellow box that appears.

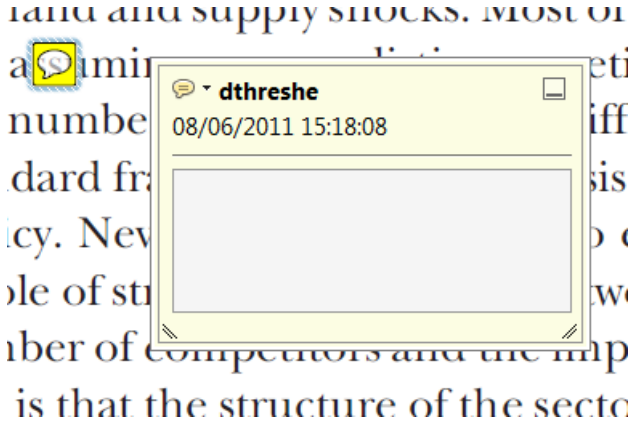

WILEY-BLACKWELL

USING e-ANNOTATION TOOLS FOR ELECTRONIC PROOF CORRECTION

5. Attach File Tool – for inserting large amounts of text or replacement figures.

Inserts an icon linking to the attached file in the appropriate pace in the text.

How to use it

- Click on the Attach File icon in the Annotations section.
- Click on the proof to where you'd like the attached file to be linked.
- Select the file to be attached from your computer or network.
- Select the colour and type of icon that will appear in the proof. Click OK.

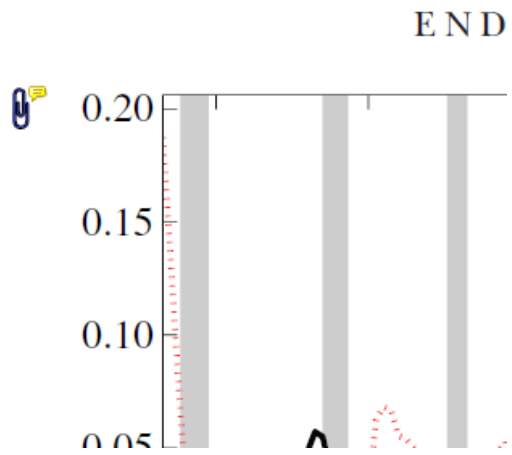

6. Add stamp Tool – for approving a proof if no corrections are required.

Inserts a selected stamp onto an appropriate place in the proof.

How to use it

- Click on the Add stamp icon in the Annotations section.
- Select the stamp you want to use. (The Approved stamp is usually available directly in the menu that appears).
- Click on the proof where you'd like the stamp to appear. (Where a proof is to be approved as it is, this would normally be on the first page).

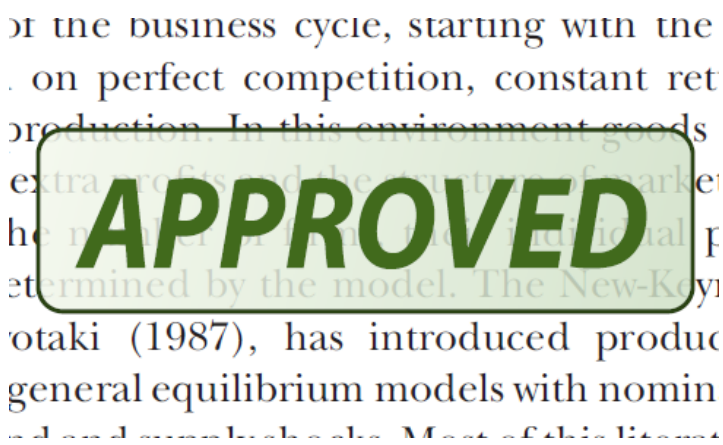

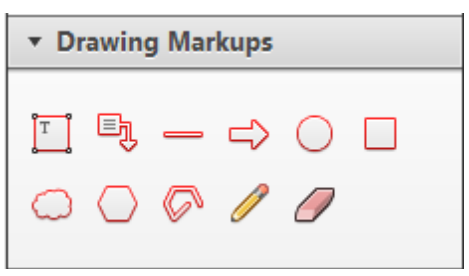

7. Drawing Markups Tools – for drawing shapes, lines and freeform annotations on proofs and commenting on these marks.

Allows shapes, lines and freeform annotations to be drawn on proofs and for comment to be made on these marks..

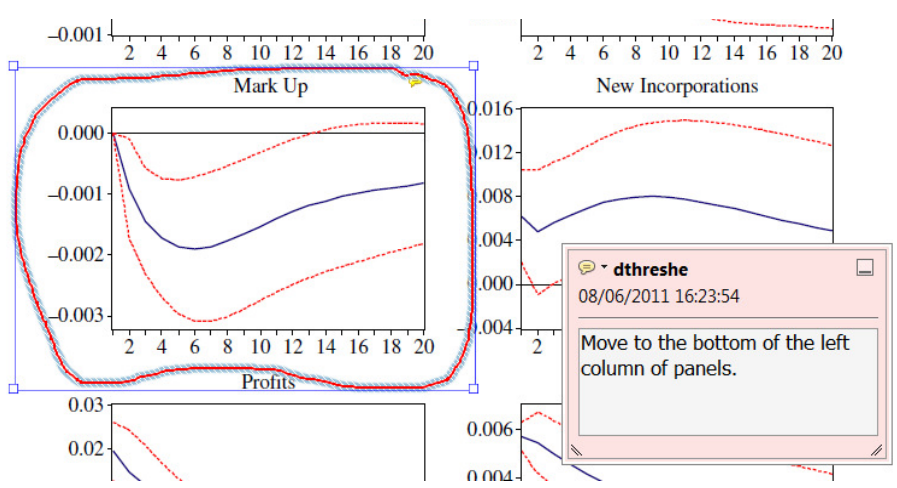

How to use it

- Click on one of the shapes in the Drawing Markups section.
- Click on the proof at the relevant point and draw the selected shape with the cursor.
- To add a comment to the drawn shape, move the cursor over the shape until an arrowhead appears.
- Double click on the shape and type any text in the red box that appears.

For further information on how to annotate proofs, click on the Help menu to reveal a list of further options: